Journal of Physics D: Applied Physics

PAPER

Tunable dielectric BIC metasurface for high resolution optical filters

IOP Publishing Journal of Physics D: Applied Physics
J. Phys. D: Appl. Phys. 56 (2023) 134002 (7pp) https://doi.org/10.1088/1361-6463/acb55d

Tunable dielectric BIC metasurface for high resolution optical filters

Fanglin Tian[1,3], **Junxiao Zhou**[1,3], **Elizabeth Abraham**[1] and **Zhaowei Liu**[1,2,*]

[1] Department of Electrical and Computer Engineering, University of California, San Diego, 9500 Gilman Drive, La Jolla, CA 92093, United States of America
[2] Materials Science and Engineering, University of California, San Diego, 9500 Gilman Drive, La Jolla, CA 92093, United States of America

E-mail: zhaowei@ucsd.edu

Received 30 September 2022, revised 13 January 2023
Accepted for publication 23 January 2023
Published 8 March 2023

Abstract
The dielectric metasurface has become a powerful tool for compact optical components with various wavefront controlling functionalities accompanied by negligible losses at the corresponding working frequencies. In this work, we propose a tunable all-dielectric metasurface as an optical filter with high resolution covering different optical communication bands, where tunability is realized by a combination of changing the incident angle and modulating the refractive index of an optical phase changing material (OPCM). When the incident angle varies, our optical filter based on a two-dimensional bound state in continuums (BIC) metasurface can achieve sequential, extremely sharp resonances. In addition, the resonance peaks could be further shifted to a different frequency band by the refractive index change of OPCM via pulsed laser heating. The proposed scheme can offer optical filters with high spectral resolution and large tunable working wavelength range, which greatly benefits from the topological property of BIC and large modulation depth of OPCM.

Keywords: tunable, metasurface, optical phase changing material, bound state in continuums, edge imaging

(Some figures may appear in colour only in the online journal)

1. Introduction

The metasurface, planar arrangements of designed sub-wavelength nanostructures, has recently emerged as a convenient, flexible, and efficient platform for electromagnetic wave manipulation [1, 2]. Due to the negligible losses at the designed wavelength, dielectric metasurfaces have recently attracted a lot of attention [3, 4]. The developed dielectric metasurfaces have been proposed for various applications including wavefront shaping [5, 6], spin manipulation [7–9], and edge imaging [10–15], just to name a few. As optical metasurfaces have become relevant for practical applications, the capability of actively modulating their optical functions is increasingly important [16–19]. For the realization of most reconfiguration metasurfaces, the essence is to dynamically shift the spectral position of the element resonances as a function of an external stimulation.

Recently, a unique group of materials, optical phase changing material (OPCM) with at least two different reversely modulated phase states, i.e. amorphous, and crystalline, have drawn a lot of attention [20–23]. With external excitation, OPCM demonstrates significant change of optical properties under different material phases, which provides an ideal platform for dynamical manipulation of active optical devices. Among them, Sb_2S_3 outperforms most other competitors benefiting from its ultra-low optical loss ($k < 10^{-5}$) at

[3] These authors contributed equally to this work.
[*] Author to whom any correspondence should be addressed.

telecommunication wavelengths, which makes it a compelling candidate in the optical industry [24].

In another context, the bound state in continuums (BIC) is a general wave phenomenon whose resonances can be perfectly confined in the system, with even the outgoing wave allowed in the surrounding environment [25, 26]. BIC was first proposed in quantum systems where the electron wave can be trapped in the designed quantum potential at an energy that would normally couple to the outgoing waves [27]. The underlying physical origin of this special localization behavior can be related to the fully decoupling between symmetry mismatched mode or the interference of radiation modes at the same location [28, 29]. The experimental realization of optical BIC devices had been done in both dielectric [30] and plasmonic [31] systems. Furthermore, BIC has been suggested for a wide range of applications in lasing [32, 33], sensing [34, 35] and filters [36, 37] due to its unique spatial confinement conditions.

In this letter, we propose a tunable optical filter based on BIC reconfigurable metasurface using Sb_2S_3 as the active medium at telecommunication wavelengths. The spectral position of resonance alters by controlling the incident angle of near infrared light and working wavelengths coverage can be further shifted through pulsed laser modulation of the refractive index change of the OPCM. Our proposed idea realizes strong near field enhancement that can be applied in biosensing with a desired value of quality (Q) factor. Benefiting from the tunable coupling strength of the quasi-BIC structure, ultrahigh-resolution spectroscopy can be achieved in the S-band, C-band and L-band with a reduced footprint.

2. Method

The wavelength and angle dependent properties (figures 2(c), (d), (g)–(i) and 3) are simulated using Lumerical Finite-Difference Time-Domain (FDTD) software. The broadband fixed angle source technique light source is employed to ensure the accurate reflectance performance of the designed quasi-BIC device under different incident angle. The light source and reflection monitor are placed far enough away from the structure to avoid any possible interference. In addition to FDTD simulations, the ideal and quasi-BIC field distribution (figures 2(e) and (f)) are simulated using the eigenfrequency solver in COMSOL Multiphysics. In both cases, the periodic boundary condition is used.

3. Results

3.1. Quasi-BIC metasurface optical filter

We exploit the near-infrared nanophotonic optical filter that reflects the high-resolution spectral peak at each different incident angle with a femtosecond (fs) laser pulse to tune the OPCM properties, thus shifting the resonance frequency. The working principle is schematically shown in figure 1(a). The metasurface structure contains a zigzag array of Sb_2S_3 bars arranged on a CaF_2 substrate and capped by the CaF_2 to keep the geometrical structure stable under thermal cycling. When a pulse laser works as an external stimulus, the angle dependent spectral peak is shifted as shown in figure 1(b), stemming from the refractive index modulation of OPCM (figure 1(c)). The working wavelength range thus can be extended to cover major telecommunication bands. The line shape of the resonances is based on the collective behavior of Fano resonances in all-dielectric metasurface driven by the physics of quasi-BIC [38]. The refractive index of Sb_2S_3 used in this work is adopted from the literature [24], as shown in figure 1(d).

The unit cell of our designed metasurface consists of two opposite oriented rectangular-shaped Sb_2S_3 bars as the active medium which is shown in figure 2(a). The capping layer CaF_2 is added on top of the Sb_2S_3 bars for protection during the laser pulse modulation, as described in figure 2(b). First, we analyse the physical origin of BIC in the designed metasurface with in-plane asymmetry. The ideal optical BIC structure devices (consider the material is lossless and the whole structure has infinite periods) support a symmetry protected state at orientation angle $\alpha = 0°$, comprise infinite value of the Q factor with vanishing optical resonance width. While in practice, most experimentally realized BIC devices can be considered as quasi-BIC due to non-ideal lossy dielectric medium, fabrication inaccuracy to partially break the spatial symmetry and finite sized structure that create additional radiation channel to external environments. The symmetry protected BICs are unstable under perturbations that break the in-plane inversion symmetry $(x, y) \to (-x, -y)$ and will transform into quasi-BIC state with finite Q factor.

As demonstrated in figure 2(c), detailed reflection spectrum under different orientation angle α are calculated. It can be observed that ideal BIC at 0° with infinite high Q degrades into quasi-BIC state with lower Q factor. The reflection line shape becomes sharper as α is smaller and disappeared at 0°, which agrees well with our analysis. Next, we examine the Q factor dependent on orientation angle provided in figure 2(d). Especially, the quadratic dependence relationship can numerically represent the behavior of quasi-BIC radiative quality factor as a function of $Q_{\text{rad}}(\alpha) = Q_0(\sin\alpha)^{-2}$, where Q_0 is a constant determined by the metasurface design [39]. Furthermore, we study the near field enhancement of the resonance mode arising from the physics of BIC states, and we choose the orientation angle $\alpha = 12°$ by considering the balance between the resonance strength and fabrication effort and 0° for ideal BIC as two examples, shown in figures 2(e) and (f). When the orientation angle $\alpha = 12°$, the sharp resonance metasurface exhibits a near field electric field enhancement $|E/E_0|$ over 80 times at resonance, and the field distribution is strongly localized near the edge of the bars. The calculated electrical field vector of the two nanobars indicated by the white arrows point to the opposite directions in figure 2(e). Figure 2(f) shows that under mirror reflection operation around y axis, the ideal BIC eigenmode and the electric field vector is changed by a factor of -1. Which indicates that in-plane

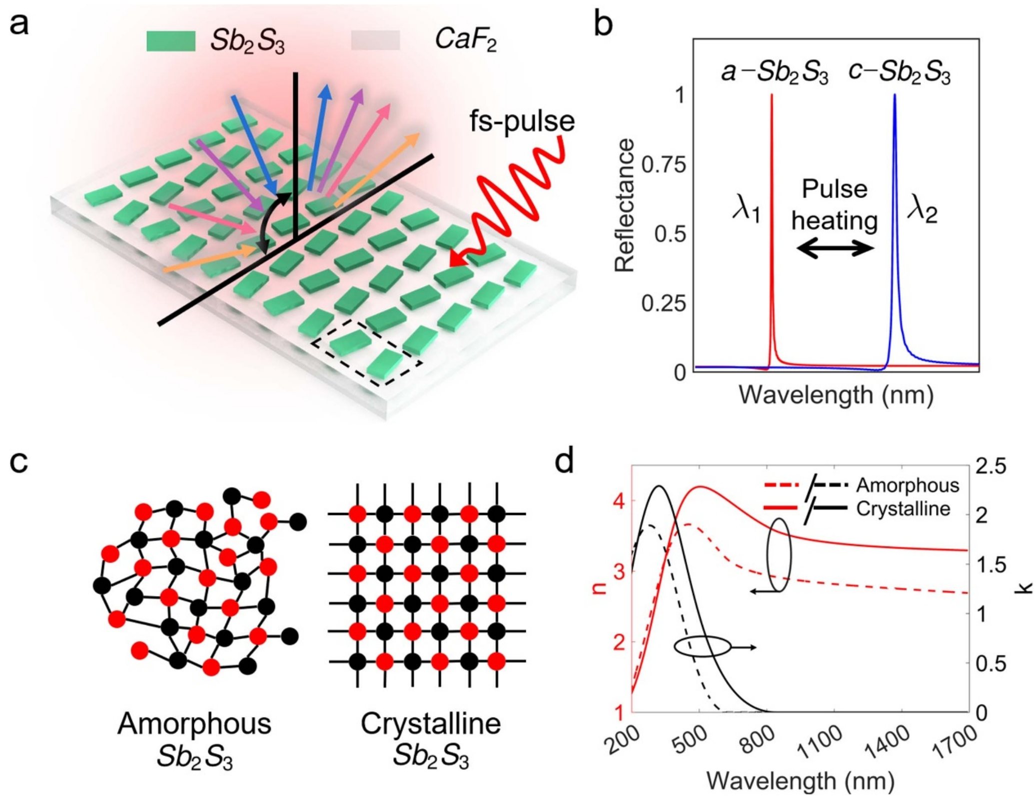

Figure 1. Concept of the OPCM based BIC metasurface for tunable filters. (a) Schematics of the proposed tunable metasurface. The unit cell of the designed metasurface (dashed rectangular) contains two rectangular Sb_2S_3 bars on top of CaF_2 substrate, where two bars point to each other at some angle. (b) Femtosecond pulse laser is used to modulate the phase of Sb_2S_3, and the central frequency of resonance is tuned over telecommunication range. (c) Schematic illustration of phase transition of Sb_2S_3 between amorphous and crystalline states. (d) The wavelength dependent optical constants of Sb_2S_3 at different material phases.

inversion symmetry is preserved compared with figure 2(e). It should be noted that this true BIC mode in figure 2(f) cannot be excited by using far-field illumination at normal incidence, unless using the near-field excitation approaches or varying the incident angle [40, 41].

Regarding the desired working band at telecommunication frequency range, the unit cell of the metasurface has been optimized with a periodicity of P_x = 970 nm and $P_y = 555$ nm. The length and width of the bar is $L_x = 210$ nm and L_y = 390 nm by considering the balance between fabrication difficulties and near-field enhancement strength. The thickness $t_{\mathrm{cap}} = 500$ nm is chosen to eliminate the background reflection as much as possible. As the height of the Sb_2S_3 bar increases, the full width half maximum of resonance increases and the background off-resonance reflection decreases. The simulated optical reflection spectra of one unit cell with various height of Sb_2S_3 bars is shown in figure 2(g), and the thickness t_{bar} = 200 nm balances the Q factor and background reflection, which satisfies our requirement best. The electromagnetic simulation software COMSOL is employed for the calculation of optical properties of the metasurface structures.

We further calculated the angular dispersion relationship of the metasurface reflection spectra in the case of orientation angle $\alpha = 12°$, as shown in figure 2(h). Note that we only consider the TE mode due to the choice of symmetry breaking method in this work. To keep the background reflection clean and high Q factor not to be affected, incident angle θ between 0° and 30° is considered in the simulation and resonance position can be tuned spectrally from 1540 nm to 1610 nm, as descripted in figures 2(h) and (i). Here, the dispersion relationship in this quasi-BIC device is mainly related to the coupling in the short axis between unit cell which can be verified from its detailed mode profile. Therefore, increasing the incident angle results in a blue shift. The Q factor around 1100 could be retrieved from the ultra-sharp Fano resonance and verified by the eigenvalue of the mode simulation. In addition, a clean unity resonance feature with ultra-low background ($\sim$2%) can be found in each reflection spectrum when the incident polarization is parallel to the long axis of the unit cell.

3.2. Switchable bandwidth under OPCM phase modulation

The working wavelengths coverage of the metasurface based optical filter can be further extended by utilizing the refractive index modulation ability of Sb_2S_3. Here, we fix the orientation angle $\alpha = 12°$ and keep all other parameters unchanged.

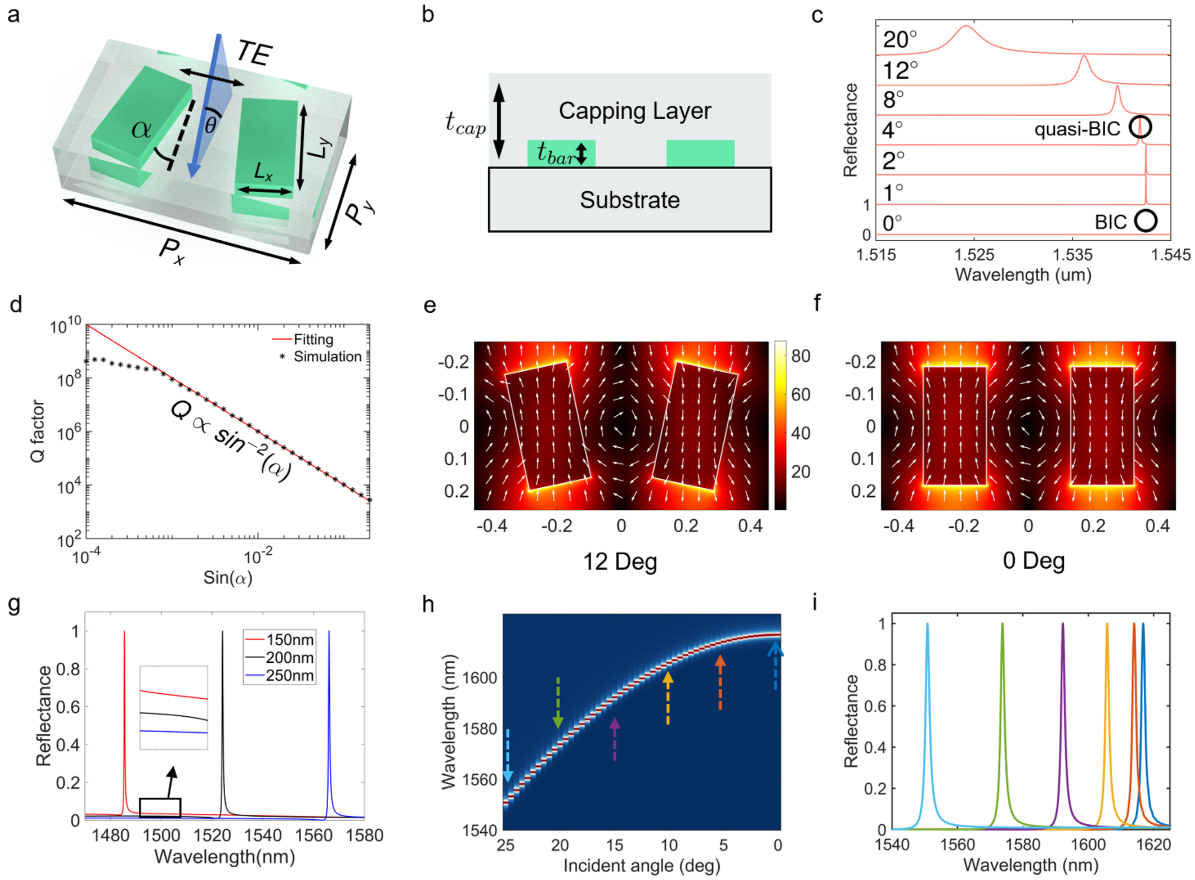

Figure 2. Working principle of quasi-BIC optical filter and performance under different conditions. (a) Schematic figure of one unit cell and incidence configuration. Only transverse electric (TE) mode is considered in this study. (b) Cross sectional view of the unit cell. The capping layer CaF_2 is used to keep the structure stable under pulsed laser modulation. (c) Evolution of the transmission spectra vs orientation angle α. (d) Dependence relationship of the Q factor on the orientation angle α. The difference between fitting curve and simulation results stems from the numerical simulation capabilities. (e) Simulated near-field electric field enhancement $|E/E_0|$ and the corresponding electrical field vector for quasi-BIC state at $\alpha = 12°$. (f) The same case with (e) but at $\alpha = 0°$, which represents the ideal BIC state. (g) Reflection spectra of the optical filter with different thicknesses of Sb_2S_3 bars. The red, black and blue curves indicate the thickness of the bar are 150 nm, 200 nm, 250 nm. Magnified reflectance between 1495 nm and 1515 nm shows in inset figure. (h) Full resonance dispersion curves under different incident angle θ with $\alpha = 12°$. The resonance shifts toward higher frequency while Q factor remains high and background reflection remains ultralow. (i) Simulated reflection spectra of the incident angle θ at 0°, 5°, 10°, 15°, 20° and 25° in transverse electric (TE) mode with orientation angle at $\alpha = 12°$.

In this condition, the spectral position of resonance peak in the optical filter is located at 1535 nm at normal incidence when the OPCM is in the amorphous state. At this wavelength, we analyze the normalized electric field (y component) and magnetic field distributions shown in figures 3(a) and (c), respectively. When the OPCM is tuned to crystalline, the same simulation is carried in figures 3(b) and (d). In addition, at incident angle $\theta = 25°$, the resonance peak shifts to 1468 nm when the OPCM is in the amorphous state. The same electric and magnetic field distribution are shown in figures 3(e)–(h).

The evolution of reflectance spectrums under different incident angles and the material phases of OPCM are shown in figure 3(i). The solid lines demonstrate the reflection spectra of the structure with Sb_2S_3 bars in amorphous condition, of which metasurface bandwidth covers the whole S-band and part of the C-band. Moreover, the dashed lines demonstrate the reflection spectra of the structure with Sb_2S_3 bars in crystalline condition, and coverage of the C-band and L-band is achieved. From the yellow curve to blue, it corresponds to the incident angles around 0°, 10.5°, 15.7°, 19.4°, 22.6°, 25.3°, respectively. Therefore, by combining the tunability of Sb_2S_3 material phase and modulation of the incident angle, the metasurface optical filter working bandwidth can fully cover the S, C and L-bands which is essential for optical telecommunication industry. Fabrication of the whole device could be done using standard cleanroom techniques including sputtering, photolithography and etching. To experimentally achieve the phase transitions between the two states, a feasible method would be to use femtosecond laser pulses with different pulse number and pulse energy [42]. Optical measurement with accurate incident angle variation could be done using a standard rotation stage.

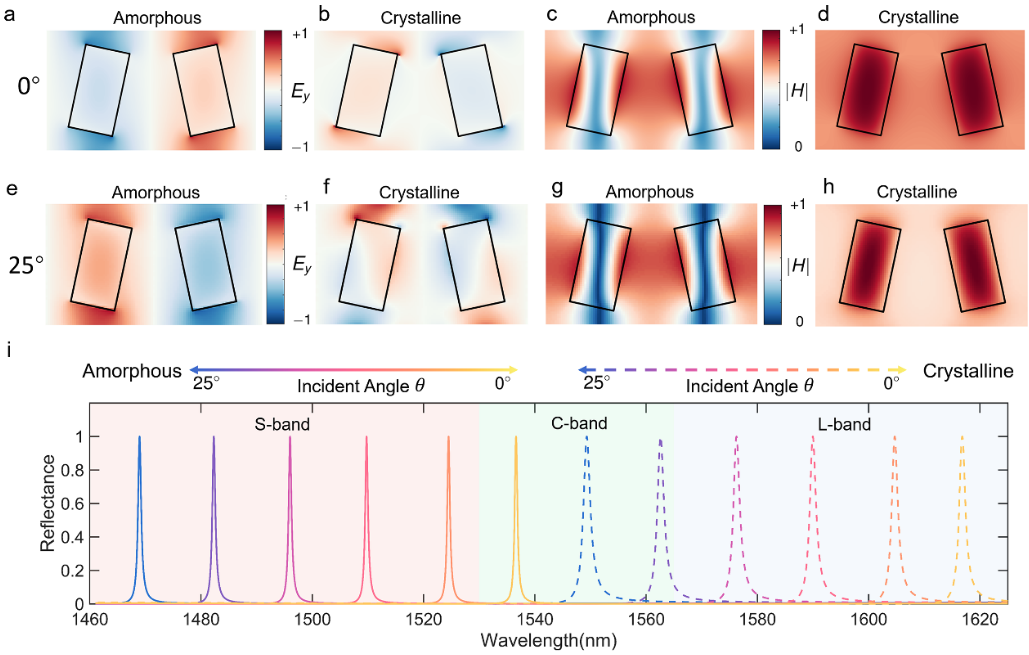

Figure 3. Tunable metasurface performance with incident angle changing and refractive index modulation. The periodicity of unit cell $P_x = 970$ nm and $P_y = 555$ nm. The size of the Sb_2S_3 bars size is fixed at $L_x = 210$ nm, $L_y = 390$ nm and $t_{\text{bar}} = 200$ nm. Orientation angle $\alpha = 12^\circ$. (a) and (b) Numerically simulated quasi-BIC for electric field (y component) when the incident angle $\theta = 0^\circ$ at 1535 nm in the case of OPCM at the amorphous state. (c) and (d) Normalized magnetic field when OPCM at the crystalline state. (e) and (f) Numerically simulated quasi-BIC for electric field (y component) when the incident angle $\theta = 25^\circ$ at 1468 nm in the case of OPCM at the amorphous state. (g) and (h) Normalized magnetic field when OPCM at the crystalline state. (i) Evolution of reflection spectra for different values of different incident angles of both amorphous and crystalline Sb_2S_3. S-band, C-band and L-band can be fully covered with smaller footprint design.

4. Discussion

It should be noted that in principle, the proposed optical filter with the whole communication band coverage could be also obtained by designing multiple metasurface arrays with different scale factors of the structure [34]. Thanks to the involvement of the OPCM with greater tunability, only one metasurface can handle it. Therefore, the complicated design requirement is reduced. We would like to emphasize that the proposed working principle could be also extended to other applications, which is highly desired of the multiple response of high Q factors, such as spectroscopy. Compared with electrical-optical system [43] and liquid crystal based optical filter [44], which can only achieve ~60% and ~90% modulation depth with Q factor being 5–10, our design realized a modulation depth around 97% and Q factor over 1000 and could be easily enhanced by decreasing the orientation angle between Sb_2S_3 nanobars. Compared with recent OPCM based filtering system [45], instead of only one-shot modulation, continuous tunability is realized varying incident angle and material phase modulation of OPCM. Moreover, the current reflection mode for high resolution optical filter could be achieved by using transmission mode, which will make the whole system more compact and easier to use for measurement. Meanwhile, it is worth mentioning that there are some limitations or shortages in our proposed design. Regarding the fabrication and structure strength, as the sharp corners in the rectangular bars could be very challenging for lithography and may not be strong enough to maintain the ultrahigh field enhancement as quality of shape may degrade during material phase modulation [46].

In conclusion, we have proposed a tunable metasurface that can serve as reflective optical filter based on the optical phase transition material Sb_2S_3 at telecommunication wavelengths. In our design, the symmetry protected quasi-BIC ensures the ultrasharp Mie resonances and unity on-resonance reflection. Furthermore, we have demonstrated the spectral position of resonance can be tuned by both the incident angle of light and phase states of Sb_2S_3. The whole working bandwidth can cover the major optical communication bands by combining the tunability of incident angle and phase modulation of Sb_2S_3 with a low background reflection as smaller as 2%. Our scheme is not just limited to optical filters, but could be further extended to spectroscope research in biology and the working wavelengths can be shifted to longer wavelengths in the near-infrared or mid-infrared using other OPCM [18, 47].

Data availability statement

The data that support the findings of this study are available upon reasonable request from the authors.

Conflict of interest

The authors declare no conflicts of interest.

Funding

Funded by the National Science Foundation (NSF-ECCS-1907423).

ORCID iD

Junxiao Zhou https://orcid.org/0000-0001-6168-8580

References

[1] Yu N and Capasso F 2014 Flat optics with designer metasurfaces *Nat. Mater.* **13** 139
[2] Kildishev A V, Boltasseva A and Shalaev V M 2013 Planar photonics with metasurfaces *Science* **339** 1232009
[3] Lin D, Fan P, Hasman E and Brongersma M L 2014 Dielectric gradient metasurface optical elements *Science* **345** 298–302
[4] Kuznetsov A I, Miroshnichenko A E, Brongersma M L, Kivshar Y S and Luk'yanchuk B 2016 Optically resonant dielectric nanostructures *Science* **354** aag2472
[5] Arbabi A, Horie Y, Ball A J, Bagheri M and Faraon A 2015 Subwavelength-thick lenses with high numerical apertures and large efficiency based on high-contrast transmitarrays *Nat. Commun.* **6** 1–6
[6] Wang Z, Li T, Soman A, Mao D, Kananen T and Gu T 2019 On-chip wavefront shaping with dielectric metasurface *Nat. Commun.* **10** 3547
[7] Zhou J, Zhang W, Liu Y, Ke Y, Liu Y, Luo H and Wen S 2016 Spin-dependent manipulating of vector beams by tailoring polarization *Sci. Rep.* **6** 34276
[8] Chen C, Gao S, Song W, Li H, Zhu S-N and Li T 2021 Metasurfaces with planar chiral meta-atoms for spin light manipulation *Nano Lett.* **21** 1815–21
[9] Liu M, Huo P, Zhu W, Zhang C, Zhang S, Song M, Zhang S, Zhou Q, Chen L and Lezec H J 2021 Broadband generation of perfect Poincaré beams via dielectric spin-multiplexed metasurface *Nat. Commun.* **12** 1–9
[10] Zhou J, Qian H, Chen C-F, Zhao J, Li G, Wu Q, Luo H, Wen S and Liu Z 2019 Optical edge detection based on high-efficiency dielectric metasurface *Proc. Natl Acad. Sci. USA* **116** 11137–40
[11] Chen M K, Yan Y, Liu X, Wu Y, Zhang J, Yuan J, Zhang Z and Tsai D P 2021 Edge detection with meta-lens: from one dimension to three dimensions *Nanophotonics* **10** 3709–15
[12] Zhou J, Qian H, Zhao J, Tang M, Wu Q, Lei M, Luo H, Wen S, Chen S and Liu Z 2021 Two-dimensional optical spatial differentiation and high-contrast imaging *Natl Sci. Rev.* **8** nwaa176
[13] Zhou Y, Wu W, Chen R, Chen W, Chen R and Ma Y 2020 Analog optical spatial differentiators based on dielectric metasurfaces *Adv. Opt. Mater.* **8** 1901523
[14] Zhou J, Liu S, Qian H, Li Y, Luo H, Wen S, Zhou Z, Guo G, Shi B and Liu Z 2020 Metasurface enabled quantum edge detection *Sci. Adv.* **6** eabc4385
[15] Zhou Y, Zheng H, Kravchenko I I and Valentine J 2020 Flat optics for image differentiation *Nat. Photon.* **14** 316–23
[16] Zhou J, Qian H, Chen C-F, Chen L and Liu Z 2020 Kerr metasurface enabled by metallic quantum wells *Nano Lett.* **21** 330–6
[17] He Q, Sun S and Zhou L 2019 Tunable/reconfigurable metasurfaces: physics and applications *Research* **2019** 1849272
[18] Zhang Y, Fowler C, Liang J, Azhar B, Shalaginov M Y, Deckoff-Jones S, An S, Chou J B, Roberts C M and Liberman V 2021 Electrically reconfigurable non-volatile metasurface using low-loss optical phase-change material *Nat. Nanotechnol.* **16** 661–6
[19] Zhou J, Zhao J, Wu Q, Chen C-F, Lei M, Chen G, Tian F and Liu Z 2022 Nonlinear Computational Edge Detection Metalens *Adv. Funct. Mater.* **32** 2204734
[20] Lencer D, Salinga M, Grabowski B, Hickel T, Neugebauer J and Wuttig M 2008 A map for phase-change materials *Nat. Mater.* **7** 972–7
[21] Zhang Y *et al* 2019 Broadband transparent optical phase change materials for high-performance nonvolatile photonics *Nat. Commun.* **10** 1–9
[22] Lu L, Dong Z, Tijiptoharsono F, Ng R J H, Wang H, Rezaei S D, Wang Y, Leong H S, Lim P C and Yang J K 2021 Reversible tuning of Mie resonances in the visible spectrum *ACS Nano* **15** 19722–32
[23] Liu H, Dong W, Wang H, Lu L, Ruan Q, Tan Y S, Simpson R E and Yang J K 2020 Rewritable color nanoprints in antimony trisulfide films *Sci. Adv.* **6** eabb7171
[24] Delaney M, Zeimpekis I, Lawson D, Hewak D W and Muskens O L 2020 A new family of ultralow loss reversible phase-change materials for photonic integrated circuits: sb_2S_3 and Sb_2Se_3 *Adv. Funct. Mater.* **30** 2002447
[25] Hsu C W, Zhen B, Stone A D, Joannopoulos J D and Soljačić M 2016 Bound states in the continuum *Nat. Rev. Mater.* **1** 1–13
[26] Wuttig M, Bhaskaran H and Taubner T 2017 Phase-change materials for non-volatile photonic applications *Nat. Photon.* **11** 465–76
[27] Von Neumann J and Wigner E 1929 Über merkwürdige diskrete Eigenwerte Phys *Phys. Z.* **30** 465–7
[28] Plotnik Y, Peleg O, Dreisow F, Heinrich M, Nolte S, Szameit A and Segev M 2011 Experimental observation of optical bound states in the continuum *Phys. Rev. Lett.* **107** 183901
[29] Gao X, Hsu C W, Zhen B, Lin X, Joannopoulos J D, Soljačić M and Chen H 2016 Formation mechanism of guided resonances and bound states in the continuum in photonic crystal slabs *Sci. Rep.* **6** 1–7
[30] Hsu C W, Zhen B, Lee J, Chua S-L, Johnson S G, Joannopoulos J D and Soljačić M 2013 Observation of trapped light within the radiation continuum *Nature* **499** 188–91
[31] Sun S, Ding Y, Li H, Hu P, Cheng C-W, Sang Y, Cao F, Hu Y, Alù A and Liu D 2021 Tunable plasmonic bound states in the continuum in the visible range *Phys. Rev.* B **103** 045416
[32] Kodigala A, Lepetit T, Gu Q, Bahari B, Fainman Y and Kanté B 2017 Lasing action from photonic bound states in continuum *Nature* **541** 196–9
[33] Ha S T, Fu Y H, Emani N K, Pan Z, Bakker R M, Paniagua-Domínguez R and Kuznetsov A I 2018 Directional lasing in resonant semiconductor nanoantenna arrays *Nat. Nanotechnol.* **13** 1042–7
[34] Tittl A, Leitis A, Liu M, Yesilkoy F, Choi D-Y, Neshev D N, Kivshar Y S and Altug H 2018 Imaging-based molecular barcoding with pixelated dielectric metasurfaces *Science* **360** 1105–9
[35] Liu Y, Zhou W and Sun Y 2017 Optical refractive index sensing based on high-Q bound states in the continuum in free-space coupled photonic crystal slabs *Sensors* **17** 1861
[36] Leitis A, Tittl A, Liu M, Lee B H, Gu M B, Kivshar Y S and Altug H 2019 Angle-multiplexed all-dielectric metasurfaces for broadband molecular fingerprint retrieval *Sci. Adv.* **5** eaaw2871

[37] Dong Z, Jin L, Rezaei S D, Wang H, Chen Y, Tjiptoharsono F, Ho J, Gorelik S, Ng R J H and Ruan Q 2022 Schrödinger's red pixel by quasi-bound-states-in-the-continuum *Sci. Adv.* **8** eabm4512

[38] Lee J, Zhen B, Chua S-L, Qiu W, Joannopoulos J D, Soljačić M and Shapira O 2012 Observation and differentiation of unique high-Q optical resonances near zero wave vector in macroscopic photonic crystal slabs *Phys. Rev. Lett.* **109** 067401

[39] Koshelev K, Lepeshov S, Liu M, Bogdanov A and Kivshar Y 2018 Asymmetric metasurfaces with high-Q resonances governed by bound states in the continuum *Phys. Rev. Lett.* **121** 193903

[40] van Hoof N J, Abujetas D R, Ter Huurne S E, Verdelli F, Timmermans G C, Sánchez-Gil J A and Rivas J G 2021 Unveiling the symmetry protection of bound states in the continuum with terahertz near-field imaging *ACS Photon.* **8** 3010–6

[41] Dong Z, Mahfoud Z, Paniagua-Domínguez R, Wang H, Fernández-Domínguez A I, Gorelik S, Ha S T, Tjiptoharsono F, Kuznetsov A I and Bosman M 2022 Nanoscale mapping of optically inaccessible bound-states-in-the-continuum *Light Sci. Appl.* **11** 20

[42] Wang Q, Rogers E T, Gholipour B, Wang C-M, Yuan G, Teng J and Zheludev N I 2016 Optically reconfigurable metasurfaces and photonic devices based on phase change materials *Nat. Photon.* **10** 60–65

[43] Aalizadeh M, Serebryannikov A E, Khavasi A, Vandenbosch G A and Ozbay E 2018 Toward electrically tunable, lithography-free, ultra-thin color filters covering the whole visible spectrum *Sci. Rep.* **8** 1–11

[44] Sharma M, Hendler N and Ellenbogen T 2020 Electrically switchable color tags based on active liquid-crystal plasmonic metasurface platform *Adv. Opt. Mater.* **8** 1901182

[45] Cao T, Zhang X, Dong W, Lu L, Zhou X, Zhuang X, Deng J, Cheng X, Li G and Simpson R E 2018 Tuneable thermal emission using chalcogenide metasurface *Adv. Opt. Mater.* **6** 1800169

[46] Agrawal A, Kriegel I and Milliron D J 2015 Shape-dependent field enhancement and plasmon resonance of oxide nanocrystals *J. Phys. Chem.* C **119** 6227–38

[47] Tittl A, Michel A K U, Schäferling M, Yin X, Gholipour B, Cui L, Wuttig M, Taubner T, Neubrech F and Giessen H 2015 Plasmonic absorbers: a switchable mid-infrared plasmonic perfect absorber with multispectral thermal imaging capability *Adv. Mater.* **27** 4526